



To cite this article: Pankaj Arora *et al* 1999 *J. Electrochem. Soc.* **146** 3543

View the [article online](#) for updates and enhancements.

ECS Toyota Young Investigator Fellowship



For young professionals and scholars pursuing research in batteries, fuel cells and hydrogen, and future sustainable technologies.

At least one \$50,000 fellowship is available annually.
More than \$1.4 million awarded since 2015!



Application deadline: January 31, 2023

[Learn more. Apply today!](#)

Mathematical Modeling of the Lithium Deposition Overcharge Reaction in Lithium-Ion Batteries Using Carbon-Based Negative Electrodes

Pankaj Arora,^{a,*} Marc Doyle,^{b,**} and Ralph E. White^{a,**}

^aCenter for Electrochemical Engineering, Department of Chemical Engineering, University of South Carolina, Columbia, South Carolina 29208, USA

^bDuPont Central Research and Development, Experimental Station, Wilmington, Delaware 19880-0262, USA

The processes that lead to capacity fading affect severely the cycle life and rate behavior of lithium-ion cells. One such process is the overcharge of the negative electrode causing lithium deposition, which can lead to capacity losses including a loss of active lithium and electrolyte and represents a potential safety hazard. A mathematical model is presented to predict lithium deposition on the negative electrode under a variety of operating conditions. The Li_xC_6 |1 M LiPF_6 , 2:1 ethylene carbonate/dimethyl carbonate, poly(vinylidene fluoride-hexafluoropropylene)| LiMn_2O_4 cell is simulated to investigate the influence of lithium deposition on the charging behavior of intercalation electrodes. The model is used to study the effect of key design parameters (particle size, electrode thickness, and mass ratio) on the lithium deposition overcharge reaction. The model predictions are compared for coke and graphite-based negative electrodes. The cycling behavior of these cells is simulated before and after overcharge to understand the effect of overcharge on extended cycling. These results can be used to establish operational and design limits within which safety hazards and capacity fade problems, inherent in these cells, can be minimized.

© 1999 The Electrochemical Society. S0013-4651(99)01-088-5. All rights reserved.

Manuscript submitted January 25, 1999; revised manuscript received May 10, 1999.

Two major issues facing lithium-ion battery technology are safety and capacity fade during cycling. A significant amount of work has been done to improve the cycle life and to reduce the safety problems associated with these cells. This includes newer and better electrode materials, lower-temperature shutdown separators, non-flammable or self-extinguishing electrolytes, and improved cell designs. The performance of these cells is based on the complex chemical and electrochemical reactions occurring during charge, discharge, and storage, many of which are irreversible and lead to changes in the performance of the cells during extended cycling. A detailed discussion of lithium-ion battery mathematical models and side reactions can be found elsewhere.¹ These complex phenomena can be understood in a more detailed manner through mathematical modeling of the full-cell sandwich.

Several mathematical models of lithium-ion cells have been published.²⁻⁶ None of these models has the capability to predict capacity fade observed in these cells. Doyle *et al.*⁴ modified their dual lithium-ion model to include film resistances on both electrodes and made direct comparisons with experimental cell data for the Li_xC_6 | LiPF_6 , ethylene carbonate/dimethyl carbonate (EC/DMC), poly(vinylidene fluoride-hexafluoropropylene)| $\text{Li}_x\text{Mn}_2\text{O}_4$ system. The discharge performance of the cells was described satisfactorily by including either a film resistance on the electrode particles or by contact resistances between the cell layers or current collector interfaces.^{4,5}

Recently Darling and Newman made the first attempt to model side reactions in lithium batteries by incorporating an electrolyte (1 M LiClO_4 in PC) oxidation side reaction into a lithium-ion battery model.⁶ Even though a simplified treatment of the oxidation reaction was used, these authors were able to make several interesting conclusions about self-discharge processes in these cells and their impact on positive electrode state-of-charge.

Present battery models, except the one by Darling and Newman, consider the "ideal behavior" of the systems, neglecting the phenomena that led to losses in capacity during repeated charge-discharge cycles. Fundamental models of capacity fade phenomena are less common because their processes are not as well understood. Also, models of failure modes in batteries are not usually applicable to a wide range of systems. However, the importance of these phenomena in the safe and efficient operation of high-energy lithium-ion batteries requires that they be incorporated into future battery models.

The goal of this work is to predict the conditions for the lithium deposition overcharge reaction on the negative electrode (graphite and coke) and to investigate the effect of various operating conditions, cell designs and charging protocols on the lithium deposition side reaction.

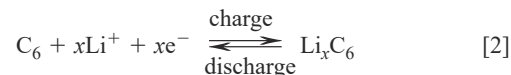
Model Development

Lithium deposition is expected to occur in lithium-ion cells due to either a higher than desired initial mass ratio, lower than expected lithium losses during the formation period, adverse charging conditions, or accidental overcharging (malfunctioning charger, malfunctioning safety circuit, or electrical misuse/abuse of the battery pack). The freshly deposited lithium covers the active surface area of the negative electrode leading to a loss of cyclable lithium and consumption of electrolyte because of the highly reactive nature of metallic lithium. This may occur at high charge rates even for cells with a conservative mass ratio because of the polarization at the negative electrode under charging conditions.⁴

However, a common circumstance leading to lithium deposition may be poorly balanced cells having too much positive electrode mass initially. Note that there is no industry standard for electrode mass ratio or anode excess for lithium-ion cells. The mass ratio (γ) of a lithium-ion cell is defined as

$$\gamma_{\text{actual}} = \frac{m_+}{m_-} = \frac{\delta_+ \epsilon_+ \rho_+}{\delta_- \epsilon_- \rho_-} \quad \gamma_{\text{theoretical}} = \frac{\Delta x C_-}{\Delta y C_+} \quad [1]$$

where γ_{actual} is the actual mass ratio and $\gamma_{\text{theoretical}}$ is the theoretical mass ratio. The intercalation-deintercalation reaction on the negative electrode (graphite or coke) may be written as



and the primary side reaction involved in the overcharge process is



The lithium metal is expected to form first near the electrode-separator boundary where the surface overpotential is greatest. Lithium metal deposited on the negative electrode reacts quickly with solvent or salt molecules in the vicinity giving Li_2CO_3 , LiF , or other insoluble products as shown in Fig. 1.^{7,8} A thin film of products (formed above) protects the solid lithium from reacting with the electrolyte.

* Electrochemical Society Student Member.

Negative Electrode (Coke or Graphite) Electrolyte (2:1 EC/DMC, 1M LiPF₆, P(VdF-HFP))

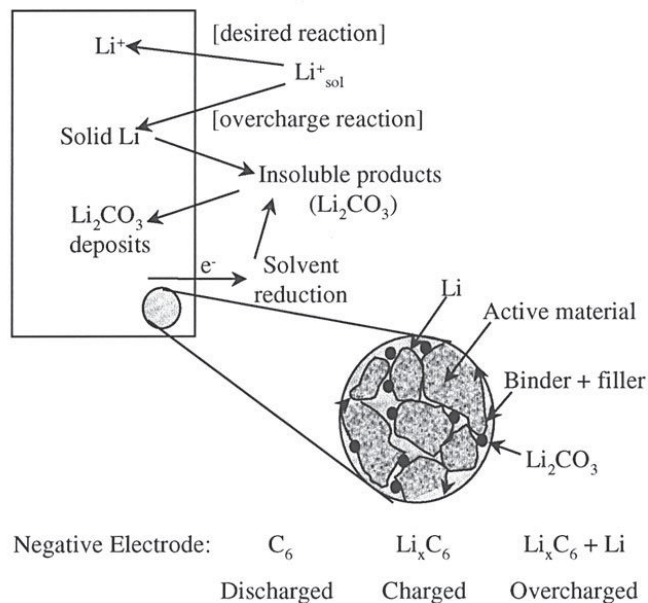
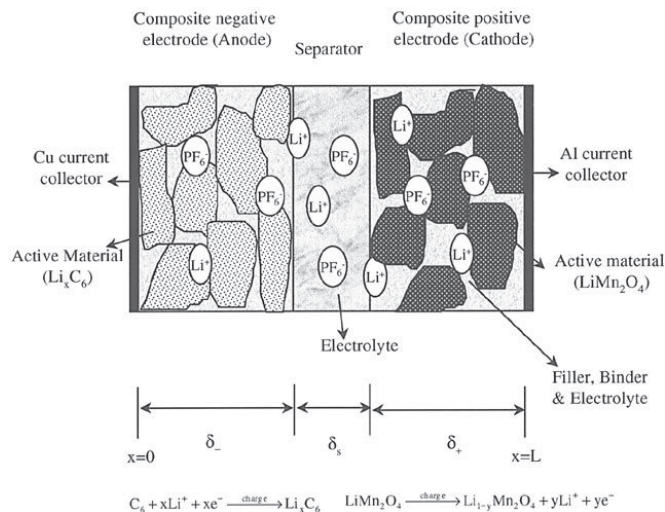


Figure 1. Reactions occurring on the negative electrode during charge and overcharge.

still dissolve during discharge. The film formed over the solid lithium is a direct loss of both active lithium and electrolyte. The products formed may block the pores, leading to a loss of rate capability as well as capacity losses. Formation of lithium metal is also a safety hazard due to its extreme reactivity with liquid solvents.

A schematic of a lithium-ion cell is shown in Fig. 2. It consists of a composite negative electrode (active material + filler + binder), separator and a composite positive electrode. The negative and positive active materials simulated in this work are graphite (MCMB 2528) and LiMn₂O₄, respectively. Other details and data for the Li_xC₆|1 M LiPF₆, EC/DMC, p(VdF-HFP)|Li_yMn₂O₄ system are given elsewhere.⁴ Lithium metal deposition may be more of a concern with graphitic carbon electrodes than with coke electrodes due to the lower average open-circuit potential of the former. For this reason, mass ratios in cells using graphite are usually chosen to be much smaller than the optimum in order to provide a buffer against lithium deposition, with the consequence that the full 372 mAh/g capacity of the graphite is not utilized. The model predictions for



graphite-based negative electrodes are compared with coke-based negative electrodes.

The main side reaction in the negative electrode during overcharge is given by Eq. 3, which can be written in general notation as⁹



The rate of the lithium deposition reaction is charge-transfer-kinetic controlled and can be expressed by a Butler-Volmer expression as follows

$$i_k = i_{o,k} \left[\exp\left(\frac{\alpha_{a,k} F}{RT} \eta_{s,k}\right) - \exp\left(-\frac{\alpha_{c,k} F}{RT} \eta_{s,k}\right) \right] \quad [5]$$

A number of different approximations can be made to simplify the computational process while including the lithium metal deposition side reaction. Either a Tafel or linear approximation to the Butler-Volmer rate expression can be used depending on the reaction conditions and simplifying assumptions. The cathodic Tafel expression can be used to describe the rate expression if either the deposition reaction is considered to be irreversible or if the amount of lithium deposited is very small and reacts quickly with the solvent. In that case, the rate expression will be

$$i_k = -i_{o,k} \exp\left(-\frac{\alpha_{c,k} F}{RT} \eta_{s,k}\right) \quad [6]$$

The lithium deposition reaction is a facile process under many conditions; the surface overpotentials may be sufficiently low that the reaction can be expressed adequately using the linear approximation

$$i_k = i_{o,k} \frac{(\alpha_{a,k} + \alpha_{c,k}) F}{RT} \eta_{s,k} \quad [7]$$

In this work, we have assumed that the lithium deposition reaction is semireversible, *i.e.*, at least part of the deposited lithium can dissolve during discharge. Some amount of the lithium may react with the electrolyte to form insoluble products such as Li₂CO₃, etc. A cathodic Tafel rate expression is also incorporated in the model and model predictions will be compared for both cases (Butler-Volmer and Tafel rate expression). In the above expressions (Eq. 5, 6, and 7), *i*_{o,k} is the exchange-current density and $\eta_{s,k}$ is the local value of surface overpotential defined by

$$\eta_{s,k} = \phi_1 - \phi_2 - U_k - F j_{n,k} R_{\text{film}} \quad [8]$$

where *U*_k is the open-circuit potential. The potential variables ϕ_1 and ϕ_2 represent the potentials in the solid and solution phases, respectively, and *i*_{o,k}, $\alpha_{a,k}$, and $\alpha_{c,k}$ are the kinetic parameters. Here

$$\alpha_{s,k} + \alpha_{c,k} = 1 \quad [9]$$

Based on the above discussion and assumptions, application of Eq. 5 to reactions 2 and 3 results in the following kinetic expressions

$$j_{n,1} = \frac{i_{0,1}}{F} \left[\frac{\exp\left(\frac{\alpha_{a,1} F}{RT} [\phi_1 - \phi_2 - U_1(c_s) - F j_{n,1} R_{\text{film}}]\right)}{\exp\left(-\frac{\alpha_{c,1} F}{RT} [\phi_1 - \phi_2 - U_1(c_s) - F j_{n,1} R_{\text{film}}]\right)} \right] \quad [10]$$

and

$$j_{n,2} = \frac{i_{0,2}}{F} \left[\frac{\exp\left(\frac{\alpha_{a,2} F}{RT} [\phi_1 - \phi_2 - U_2 - F j_{n,2} R_{\text{film}}]\right)}{\exp\left(-\frac{\alpha_{c,2} F}{RT} [\phi_1 - \phi_2 - U_2 - F j_{n,2} R_{\text{film}}]\right)} \right] \quad [11]$$

where *j*_{n,1} and *j*_{n,2} correspond to the rates of the lithium intercalation

rent density is related to the pore wall flux by $i_n = Fj_n$. The open-circuit potential U_2 is equal to zero because we are measuring the potential with respect to a lithium metal reference electrode in solution at the same local concentration. R_{film} ($\Omega \text{ cm}^2$) is a resistance caused by the film formed over the electrode surface. The resistance of the film is treated by modifying the Butler-Volmer kinetic expression for the insertion reaction and the lithium deposition reaction as shown in Eq. 10 and 11. The exchange-current densities for the insertion reaction ($i_{0,1}$) and lithium deposition reaction ($i_{0,2}$) have the form

$$i_{0,1} = F(k_{a,1})^{\alpha_{c,1}}(k_{c,1})^{\alpha_{a,1}}(c_t - c_s)^{\alpha_{a,1}}(c_s)^{\alpha_{c,1}}(c)^{\alpha_{a,1}} \quad [12]$$

$$i_{0,2} = F(k_{a,2})^{\alpha_{c,2}}(k_{c,2})^{\alpha_{a,2}}(c)^{\alpha_{a,2}} \quad [13]$$

The open-circuit potential U_1 is a function of the amount of lithium inserted and can be described by Eq. 14 for mesocarbon (MCMB) 2528⁴

$$U_1 = 0.7222 + 0.13868x + 0.028952(x^{0.5}) - 0.017189 \left(\frac{1}{x} \right) + 0.0019144 \left(\frac{1}{x^{1.5}} \right) + 0.28082 \exp[15(0.06 - x)] - 0.79844 \exp[0.44649(x - 0.92)] \quad [14]$$

where x is c_s/c_t . The kinetic and thermodynamic parameters used to simulate the electrochemical reactions on the negative electrode are summarized in Table I. According to Jasinski *et al.*¹⁰ Li/Li⁺ has a high exchange current density in 1 M LiClO₄-PC, at least on the order of 2 to 5 mA/cm² for a smooth surface and a cathodic transfer coefficient ranging from 0.66 to 0.72. The exchange current density for lithium deposition as reported by Verbrugge is 31.6 mA/cm² and the cathodic transfer coefficient is 0.67.^{11,12} In this work, the value of exchange current density is varied from 0.1 to 3 mA/cm² to examine its effect on overcharge.

The pore-wall flux $j_{n,k}$ is defined as the reaction rate per unit volume of the porous electrode and is equal to the divergence of the current density in solution

$$\frac{1}{F} \nabla i_2 = \sum_k a j_{n,k} \quad [15]$$

The pore-wall flux across the interface is related to the flux of lithium ions into the solid phase by the boundary condition

$$j_{n,1} = -D_s \frac{\partial c_s}{\partial r} \text{ at } r = R_s \quad [16]$$

A material balance on solid lithium can be expressed as

$$\frac{\partial c_i}{\partial t} = -\nabla N_i + R_i \quad [17]$$

where R_i is the production rate of species i per unit volume of the electrode due to the electrochemical reaction

$$R_i = -\frac{s_{i,k} a}{n_k F} i_{n,k} \quad [18]$$

For solids such as metallic lithium, the flux will be zero to a very good approximation. Thus the mass balance on the solid lithium reduces to

$$\frac{\partial c_{\text{Li}}}{\partial t} = -a \frac{i_{n,2}}{F} \quad [19]$$

where c_{Li} is the moles of lithium metal per volume of electrode, and a is the surface area to volume ratio as defined below for spherical carbon particles

$$a = \frac{3(1 - \epsilon_l - \epsilon_p - \epsilon_f)}{R_s} \quad [20]$$

By assuming that the negative-electrode particles are spherical in nature, the rate of the side reaction can be related to the growth of a film on the surface of the electrode particles according to

$$\frac{\partial \delta_{\text{film}}}{\partial t} = -\frac{i_{n,2} M}{\rho F} \quad [21]$$

where δ_{film} is the film thickness composed of solid lithium and other products and M and ρ are the molecular weight and density of lithium and products. The resistance [$R_{\text{products}}(t)$] of the film formed by lithium and other products (Li₂CO₃ is used as an example here) is given by

$$R_{\text{products}}(t) = z_{\text{Li}} \left(\frac{\delta_{\text{film}}}{\kappa_{\text{Li}}} \right) + z_{\text{Li}_2\text{CO}_3} \left(\frac{\delta_{\text{film}}}{\kappa_{\text{Li}_2\text{CO}_3}} \right) \quad [22]$$

where z_{Li} and $z_{\text{Li}_2\text{CO}_3}$ are the volume fractions of lithium and Li₂CO₃ present in the film. The film resistance in Eq. 8 is given by

$$R_{\text{film}} = R_{\text{SEI}} + R_{\text{products}}(t) \quad [23]$$

for the negative electrode, where R_{SEI} corresponds to the resistance offered by the solid electrolyte interface (SEI) layer formed on the negative electrode active material during the formation period.

Recently Peled *et al.* proposed a complex two-layer multicomponent structure for the SEI layer formed on lithium and lithiated carbon electrodes.¹³ According to these authors, the inner layer (closer to the negative electrode) is rich in Li₂O and LiF and low in Li₂CO₃, whereas the outer layer consists of 13% Li₂CO₃ and other semicarbonates, 10% LiF, and the remainder polyolefins. In order to simplify the present mathematical model, the composition of the film formed during overcharge is assumed to consist of only Li and Li₂CO₃ in a single layer.

The mathematical model requires a number of physical properties. The design adjustable parameters and other parameters for the electrodes are given in Tables I, II, and III. The mathematical equations describing the electrochemical reactions, mass transport, and other physical processes within the cell are discussed in detail in Ref. 2 and 3. This nonlinear system of six independent governing equations and six dependent variables (c , ϕ_2 , c_s , i_2 , j_n , ϕ_1) is solved using Newman's BAND subroutine.⁹

Table I. Kinetic and thermodynamic parameters.

Parameters	Intercalation reaction (Eq. 1) Value	Deposition reaction (Eq. 2) Value
i_0 (mA/cm ²)	0.21 ^a	1.0 ¹⁰
α_a	0.5 ^b	0.3
α_c	0.5 ^b	0.7 ^{10,11}
n	1	1
U (vs. Li/Li ⁺)	See Eq. 14 ⁵	0.0

^a Calculated at initial conditions

Table II. Parameters for the electrodes.

Parameter	Li _x C ₆	Li _y Mn ₂ O ₄
D_s (cm ² /s)	2.0×10^{-10}	1.0×10^{-9}
σ_o (S/cm)	1.0	0.038
i_0 (mA/cm ²)	0.21	0.13
c (mol/dm ³)	30.54	22.86

Table III. Design-adjustable parameters.

Parameter	Li _x C ₆	Li _y Mn ₂ O ₄
δ (μm)	99 (19% ECE ^a) 85 (5% ECE ^a) 80 (0% ECE ^a)	179.3
R_s (μm)	12.5	8.5
c_s^0 (mol/dm ³)	21.5	3.92
ϵ_1	0.360	0.416
δ_{cc} (μm)	13.6	16.0
T ($^{\circ}\text{C}$)	21.0	
c^0 (mol/dm ³)	1.00	
δ_s (μm)	76.2	
ϵ_{1s}	0.593	
ϵ_{ps}	0.266	
ϵ_{SiO_2}	0.141	
ρ_1 (g/cm ³)	1.320	
ρ_p (g/cm ³)	1.750	

^a Excess carbon electrode.

Results and Discussion

Lithium deposition is observed on carbon-based negative electrodes when lithium-ion cells are overcharged. To minimize the lithium deposition reaction most lithium-ion cells are manufactured with excess negative electrode (excess capacity). That is, if a lithium-ion cell consists of a positive electrode and negative electrode of equal reversible cyclable capacity, then at the end of charge (or at the beginning of overcharge) most of the applied current would go to the lithium deposition side reaction on the negative electrode. However, if excess negative electrode is present, then at the end of charge the negative electrode will still be undergoing the normal charging process (lithium intercalation). The lithium lost during lithium deposition may lead to changes in the capacity balance (Eq. 1).

For optimum performance, the ratio of the lithium-ion capacities of the two host materials should be balanced. The actual mass ratio calculated for the cell [mesocarbon microbead (MCMB) 2528/LiMn₂O₄] modeled in this study is 2.47. The theoretical mass ratio calculated on the basis of the theoretical capacity of the positive (148 mAh/g) and negative electrodes (372 mAh/g) is 3.03 when using $\Delta x = 1.0$ and $\Delta y = 0.83$. This leads to the conclusion that an excess of 18.6% capacity exists in the negative electrode. Considering also the irreversible capacity on the negative electrode (which can be 8-12% for MCMB type graphite), it is apparent that a wide safety margin exists to prevent accidental lithium deposition on the graphite during charging. In commercial cells where other safety features would exist, cells might be designed differently to provide even higher energy densities by using a larger mass ratio closer to the theoretical value. On changing the thickness of the negative electrode to 80 and 85 μm , the excess capacity in the cell reduces to 0 and 5%, respectively. The excess capacity in this work is defined as

$$\text{Excess capacity (\%)} = \left(\frac{\gamma_{\text{theoretical}} - \gamma_{\text{actual}}}{\gamma_{\text{theoretical}}} \right) 100\% \quad [24]$$

Figure 3 shows the simulated reaction rates at the negative electrode/separators interface for the lithium intercalation and lithium deposition reactions as a function of charge time. The cell was charged galvanostatically at 2.906 mA/cm² (ca. 1 C rate) to a cutoff voltage of 4.45 V. The overpotential on the negative electrode is also shown as a function of charge time. The dashed line at 0.0 V (vs. Li/Li⁺) shows the lithium deposition potential. It is clear from the figure that no lithium was deposited even when the cell was overcharged to 4.45 V because the cell had 19% excess negative electrode. The excess negative electrode makes the cell safer but compromises the performance of the cell. It also leads to larger irre-

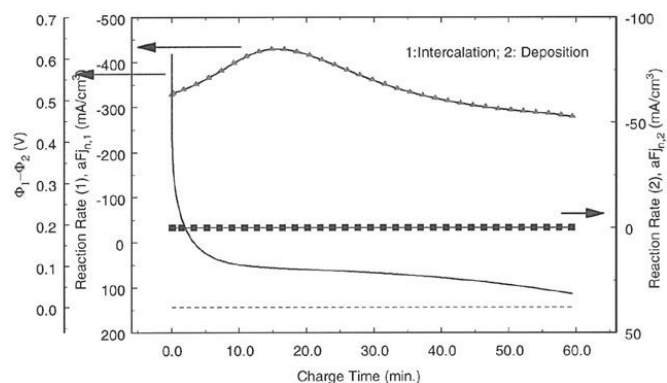


Figure 3. Simulated reaction rates as a function of charge time for 19% excess negative electrode (graphite). The cell is charged at 2.9 mA/cm² to 4.45 V and the results are shown at the negative electrode/separators interface.

The excess negative electrode active material used in commercial cells is often small to reduce the irreversible capacity loss to a minimum during the formation period. This improves the performance, but compromises the safety of these cells. Figure 4 shows the lithium deposition reaction as a function of charge time when the excess negative electrode is reduced to 5%. As soon as the overpotential on the negative electrode reaches zero, the lithium deposition reaction becomes favorable. The rate of the lithium deposition reaction compared to that of lithium intercalation is very high at this location in the cell, and leads to a large amount of deposition within a short time. The cells with no excess negative electrode will be more prone to deposition compared to cells with excess negative electrode. Lithium deposition will also start earlier (53 min for 0% excess anode, 57 min for 5% excess anode) in the absence of any excess negative electrode. The excess negative electrode clearly has a major effect on reducing the lithium deposition overcharge reaction.

Figure 5 shows the effect of charge cutoff voltage on the lithium deposition and intercalation rates. The cells were overcharged to three different cutoff voltages (4.25, 4.35, and 4.45 V) at 2.906 mA/cm² with 5% excess negative electrode. As expected, the lithium deposition reaction rate is higher when the cells are charged to higher cutoff voltages. The lithium deposition reaction dominates as soon as it begins, leading to an increase in the deposition rate and decrease in the intercalation rate. This problem becomes worse as the charging rate is increased. The value of the exchange current density for the lithium deposition/dissolution reaction as reported in the literature varies by two orders of magnitude.^{10,11} The large variation in values reported in the literature is likely due to the surface condition of the lithium under study. Freshly deposited lithium will have a high exchange current density compared to lithium covered with more-developed surface

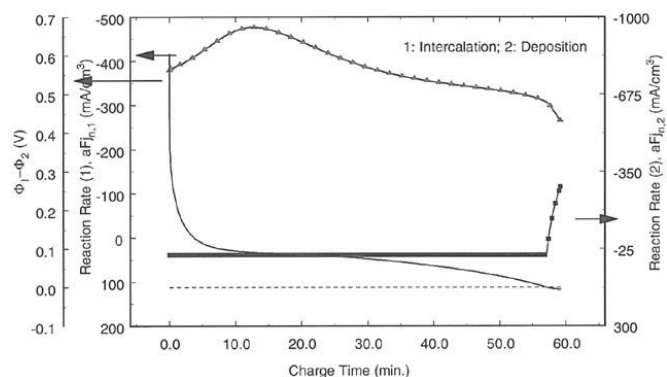


Figure 4. Simulated reaction rates as a function of charge time for 5% excess negative electrode (graphite). The cell is charged at 2.9 mA/cm² to 4.45 V

Explore Litigation Insights

Docket Alarm provides insights to develop a more informed litigation strategy and the peace of mind of knowing you're on top of things.

Real-Time Litigation Alerts



Keep your litigation team up-to-date with **real-time alerts** and advanced team management tools built for the enterprise, all while greatly reducing PACER spend.

Our comprehensive service means we can handle Federal, State, and Administrative courts across the country.

Advanced Docket Research



With over 230 million records, Docket Alarm's cloud-native docket research platform finds what other services can't. Coverage includes Federal, State, plus PTAB, TTAB, ITC and NLRB decisions, all in one place.

Identify arguments that have been successful in the past with full text, pinpoint searching. Link to case law cited within any court document via Fastcase.

Analytics At Your Fingertips



Learn what happened the last time a particular judge, opposing counsel or company faced cases similar to yours.

Advanced out-of-the-box PTAB and TTAB analytics are always at your fingertips.

API

Docket Alarm offers a powerful API (application programming interface) to developers that want to integrate case filings into their apps.

LAW FIRMS

Build custom dashboards for your attorneys and clients with live data direct from the court.

Automate many repetitive legal tasks like conflict checks, document management, and marketing.

FINANCIAL INSTITUTIONS

Litigation and bankruptcy checks for companies and debtors.

E-DISCOVERY AND LEGAL VENDORS

Sync your system to PACER to automate legal marketing.